NJC

Accepted Manuscript

ROYAL SOCIETY OF CHEMISTRY

rsc.li/njc

View Article Online
DOI: 10.1039/C7NJ00764G

Journal Name

ARTICLE

Novel environmentally sustainable synthesis of Au-Ag@AgCl nanocomposites and their application as an efficient and recyclable catalyst for quinoline synthesis

Received 00th January 20xx,
Accepted 00th January 20xx

DOI: 10.1039/x0xx00000x

www.rsc.org/

Kanti Sapkota[a,b] Sung Soo Han[a,b]*

This paper reports a facile, additive free, cost effective, green approach to the synthesis of Au-Ag@AgCl nanocomposites (NCs) using tuber extract of *Nephrolepis cordifolia*. Au-Ag@AgCl NCs were fabricated by reducing cationic Ag and Au and simultaneously generating AgCl in presence of plant material. The sizes of dispersed NCs ranged from 10 to 50 nm (average diameter 30 nm). The synthesized NC was found to catalyze multicomponent domino annulation-aromatization for quinoline synthesis. UV–visible spectroscopy, Fourier transform infrared (FT-IR) spectroscopy, powder X-ray diffraction (XRD), X-ray photoelectron spectroscopy (XPS), transmission electron microscopy (TEM), energy-dispersive X-ray (EDX) spectroscopy and thermogravimetric analysis (TGA) were used to determine the optical activity, functional groups present, crystallinity, size, oxidation state, weight loss and thermal stability, respectively, of biosynthesized Au-Ag@AgCl NCs. These NCs exhibited excellent catalytic activities and high yields when used to synthesize pharmaceutically important quinolines *via* the three-component coupling/hydroarylation/dehydrogenation of arylaldehyde, aniline, and phenyl acetylene derivatives. The nanocatalyst was easily recovered and recycled five times without significant loss of catalytic activity.

Introduction

Metallic nanoparticles have been used in catalysis, electronics, and in biological, chemical, optical, and biomedical fields. They exhibit wide ranging properties, including anticancer, antimicrobial, antidiabetic, antioxidant, and antibacterial activities,[1-4] and have even been used for wastewater treatment.[5] Chemical methods have generally been used to synthesize metallic nanoparticles, but the utilization of harmful and hazardous chemicals for chemical synthesis causes environmental pollution and raises toxicity concerns. Therefore, there is a need for environmentally benign methods for the production of nanomaterials to diminish environmental impacts and safety concerns.[6-11] Plant materials can be used for the green preparation of various metallic nanoparticles,[12-15] and they have the advantages of being readily available, environmentally sustainable, economical, and renewable. Furthermore, the chemicals present in plant materials act as reducing and stabilizing agents for the synthesis of metallic nanoparticles.[16-18]

In particular, bimetallic hybrid NCs exhibit distinct, unique characteristics as compared with their components. Hybrid metal nanoparticles not only provide the multifunctionality endowed by their components, but can also exhibit synergistic effects. Moreover, these nano materials have remarkable catalytic and optical properties.[19-22] In particular, Au–Ag based alloyed bimetallic nanoparticles have unique composition-tunable plasmonic properties that can be utilized in sensor and catalytic systems. Due to the importance and perceived potentials of these bimetallic nanomaterials, various efforts were devised for their synthesis. Recently, porous Au-Ag alloy particles decorated AgCl on-chip membranes were produced *via* a two-step facile immersion reaction and annealing process and the synthesis of one dimensional Ag/Au/AgCl NCs from Ag nanowires has also been reported.[23,24] Very recently, alloyed crystalline Au-Ag hollow nanostructures exhibiting high catalytic performance and structural and chemical stabilities were described.[25] In addition, the synthesis of monodispersed Au, Ag, and Au-Ag alloy nanoparticles using a hot-colloidal method was reported.[26] Other recent studies described the size-controlled synthesis of Au@Ag core–shell nanoparticles capped with citrate and the eco-friendly synthesis of bimetallic Au-Ag nanoparticles.[27,28] A number of authors have described the efficient synthesis of Au@AgCl or Ag@AgCl hybrid nanoparticles,[29-35] but no report has yet described the facile, efficient, ecofriendly synthesis of Au-Ag@AgCl nanomaterials. Hence, the described green synthesis of Au-Ag@AgCl NCs is novel, highly efficient, cost-effective, environmentally sustainable, and compatible for catalytic, biomedical and industrial applications.

[a]*School of Chemical Engineering, Yeungnam University, 280 Daehak-Ro, Gyeongsan, Gyeongbuk 38541, Republic of Korea*

[b]*Department of Nano, Medical & Polymer Materials, College of Engineering, Yeungnam University, 280 Daehak-Ro, Gyeongsan, Gyeongbuk 38541, Republic of Korea*

Email: sshan@yu.ac.kr
Tel: +82–53–810–2773; Fax: +82–53–810–4686

† Electronic Supplementary Information (ESI) available: [^{1}H NMR and ^{13}C NMR of the synthesized compounds]. See DOI: 10.1039/x0xx00000x

View Article Online
DOI: 10.1039/C7NJ00764G

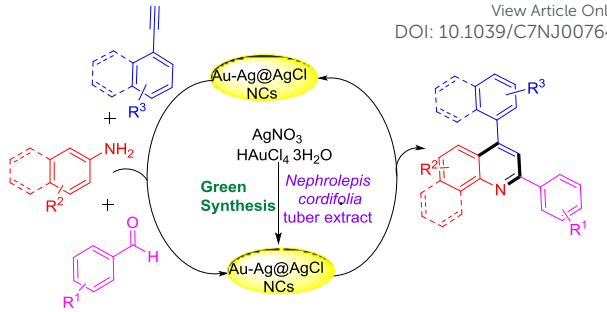

Scheme 1 Green synthesis of recyclable Au-Ag@AgCl NCs and their catalytic activity on multicomponent domino annulation-aromatization for quinoline synthesis.

Nephrolepis cordifolia belongs to the family *Nephrolepidaceae* and commonly known as the erect sword fern or tuber sword fern. It has suberect rhizomes with small hairy tubers, and is widely distributed throughout Asia and Australia. The tubers of *Nephrolepis cordifolia* are used as a traditional medicine for the treatment of coughs, fever, and hematuria and its oil exhibits cytotoxic, antibacterial, and antifungal activities. Furthermore, reported GC/MS analysis of volatile chemical constituents of *Nephrolepis cordifolia* demonstrates that it contains several bioactive molecules, such as, phytol (3.93%), α- cadinol (3.30%), thymol (0.42%), ethyl linolenate (6.33%), β-ionone (5.59%), ethyl stearate (3.19%), methyl oleate (0.54%), ethyl palmitate (8.0%), α-cadrene epoxide (1.48%), methyl palmitate (1.54%), dibutyl phthalate (1.85%),benzyl butyl phthalate (1.34%) and dibenzofuran (0.77%).[36] (Table S1 ESI†).

Electron rich compounds especially polyols and phenolic hydroxyl compound can be used as reducing or capping agents for the synthesis of nanoparticles from metal ions, and phenolic components can chelate metal ions by donating electron and be used to produce metal nanoparticles.[37,38]

Nitrogen containing heterocycles are important natural products and can be pharmaceutically active. In particular, the quinoline nucleus is present in many natural products, biologically active molecules, and functional materials,[39-44] and has been found to be associated with wide ranging pharmaceutical activities, such as, anticancer, antimalarial, antimicrobial, antituberculosis, and anti-HIV activities.[45-48] Functionalized quinolines can also be used as fluorophores and potential organic semiconductors.[49,50] Because of their importance and usefulness in diverse fields, the syntheses of quinolines have attracted the interest of synthetic organic chemists.[51-55] Representative reported reactions of quinoline synthesis include: the Skraup, Povaron, Friedlander, Doebner-Von Miller, Combes and Conrad-Limpach reactions.[56,57] Although a number of valuable approaches have been developed to construct quinolines, the limitations of existing synthetic methodologies, such as, limited availability of starting materials, costs of catalysts, harsh reaction conditions, and lower yields, new synthetic methods are required to produce quinolines. To the best of our knowledge, no previous report has described the synthesis of polyfunctionalized quinoline derivatives using environmentally compatible and recyclable Au-Ag@AgCl nano-catalyst from commercially available arylaldehyde, aniline and phenyl acetylene derivatives.

Herein, we report an efficient, facile and green synthetic route for the fabrication of Au-Ag@AgCl NCs using the tuber extract of *Nephrolepis cordifolia* as a reducing and stabilizing agent. The synthesized nanoparticles were used as recyclable, efficient catalysts for the multicomponent tandem synthesis of various quinoline derivatives from arylaldehyde, aniline, and phenyl acetylene derivatives (Scheme 1).

Experimental

Materials and methods

Gold (III) chloride trihydrate ($HAuCl_4 \cdot 3H_2O$, 99.9%), silver nitrate ($AgNO_3$, 99%), aniline, phenyl acetylene and aldehyde derivatives were purchased from Sigma-Aldrich. The air dried tubers of *Nephrolepis cordifolia (L.) C. Presl* was obtained from the Kaski district of Nepal. All purchased chemicals were used without further purification. Double distilled water was used throughout the experiments. The glassware used was cleaned with aqua-regia (3:1 concentrated solution of HCl: HNO_3), rinsed with distilled water and dried in an oven. The tubers of *Nephrolepis cordifolia* were washed with distilled water and dried at room temperature. Then, 10 gram of tuber was cut into small pieces and 100 mL of sterile water was added. The mixture was boiled for 15 minutes with continuous stirring, centrifuged at 3000 rpm for 10 minutes, and filtered.

Synthesis of Au-Ag@AgCl NCs

10 mL of prepared tuber extract was mixed with 100 mL of 1 mmol aqueous $AgNO_3$ solution in a 100 mL sterile Erlenmeyer flask, stirred for 5 min, and sonicated for 30 min when the color of the solution turned dark yellow indicating the formation of silver nanoparticles. At the same time, 10 mL of tuber extract was added to 100 ml of 1 mmol of an aqueous solution of $HAuCl_4$ in a 500 mL sterile Erlenmeyer flask and sonicated for 30 min when the color of the solution became pink/red, indicating the formation of Au nanoparticles. The dark yellow colored solution of Ag nanoparticles was then mixed with the gold nanoparticle solution. This mixture was then sonicated for 4 hours at 50 ^{o}C and kept in sunlight for 1 hr when the color of the mixture became reddish orange, indicating the formation of Au-Ag@AgCl NCs. AgCl was supposed to be generated *in situ* in the reaction mixture due to the combination of Ag^+ ions of $AgNO_3$ and Cl^- ions of $HAuCl_4$. The prepared nanoparticles were centrifuged at 10,000 rpm for 20 minutes using a Beckman coulter's centrifuge (Model: Avanti® J-E, USA), washed four times with distilled water and collected in a sterile Petri dish. Finally, they were vacuum dried in an oven for 20 hours at 50 ^{o}C. Alternatively, we tried to make the Au-Ag@AgCl NCs in one-pot procedure using 10 mL of plant extract solution with 100 mL of 1 mmol $AgNO_3$ and $HAuCl_4$. The desired Au-Ag@AgCl NCs were formed which was confirmed by XRD and TEM analysis (See Figure S4 and Figure S5 ESI†). However, TEM analysis shows that the nanoparticles formed were more aggregated compared to sequentially synthesized Au-Ag@AgCl NCs.

Characterization of NCs

The UV-visible spectra of Au-Ag@AgCl NCs were recorded to confirm the formation of nanoparticles using an UV-visible spectrophotometer (Shimadzu UV-2600) and a quartz cuvette. Fourier transform infrared (FT-IR) spectra were examined using a Perkin–Elmer FT-IR spectrometer in transmittance mode between 400 and 4000 cm^{-1}. The crystalline properties of Au-Ag@AgCl NCs were investigated by powder X-ray diffraction using a PAN alytical X'Pert PRO MPD unit (operated at an accelerating voltage of 40 kV and 30 mA with a Cu Kα X-ray source (λ = 1.5406 Å) over the 2θ range of 20° to 90°, and using a scanning rate of 1.2° min^{-1}). The sizes and shapes of the Au-Ag@AgCl NCs produced were determined by field emission transmission electron microscopy (FE-TEM, FEI Tecnai F20). The copper grid of the TEM was dipped into prepared diluted samples three times and then dried at room temperature. X-ray photoelectron spectroscopy was used to determine surface compositions and electronic states using a Thermo Scientific K-Alpha system an Al Ka X-ray source and a ion source energy range of 100 V to 3 keV. Thermal analysis was conducted by monitoring percentage of weight loss using a differential scanning calorimeter (TG-DTA, SDT-Q600 V20.5 Build 15) in the range 30 to 800 ^{o}C using a heating rate 10 ^{o}C per minute in N_2. Zeta potential measurement was performed using a Zetasizer Nano ZS (Malvern Instrument Ltd.,UK).

Catalytic activity

The synthesized Au-Ag@AgCl NCs were used as catalysts for the synthesis of various quinoline derivatives *via* three-component coupling/hydroarylation/dehydrogenation of arylaldehyde, aniline, and phenyl acetylene derivatives.

General procedure for the syntheses of quinoline derivatives 4a-4f.

2 mol% Au-Ag@AgCl NCs and 10 mol% of p-toluenesulfonic acid (PTSA) were added to a stirred solution of aldehyde **1** (1.0 mmol), amine **2** (1.0 mmol) and alkyne **3** (1.0 mmol) in 1,2-dichloroethane (5.0 mL). The reaction mixture was refluxed for 9-12 h and the progress of the reaction was monitored by TLC. After reaction completion, the solvent was removed under reduced pressure and the residue was subjected to silica gel column chromatography to isolate the pure products **4a**-**4f**.

Results and discussion

Characterization of Au-Ag @AgCl NCs

UV-visible spectroscopy was performed to confirm the formation of NCs. The UV-visible spectra of the synthesized Au-Ag@AgCl nanoparticles exhibited the characteristic surface plasmon resonance (SPR) peak of metallic Ag and Au due to the oscillation of electrons in metal nanoparticles in an applied electromagnetic field (Figure 1a). This peak is dependent on the sizes, shapes, and the microenvironments of NCs.[37]

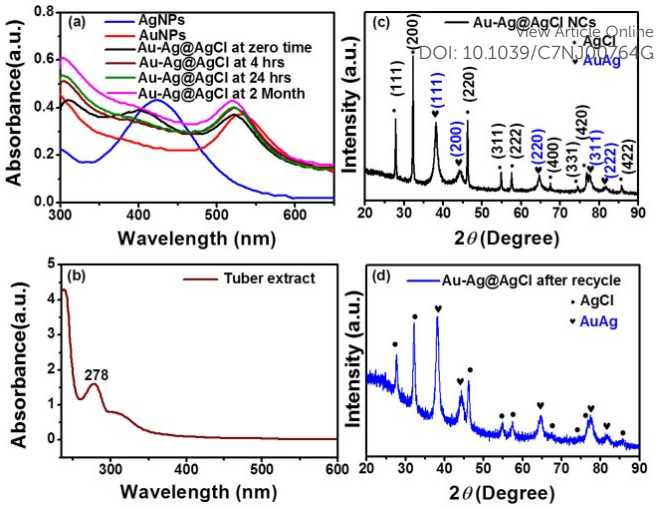

Fig. 1 UV–vis spectra and XRD patterns of Au-Ag@AgCl NCs (a) UV spectra of AuNPs, AgNPs and Au-Ag@AgCl NCs, and (b) UV spectra of *Nephrolepis cordifolia* tuber extract (c) XRD patterns of Au-Ag@AgCl (d) XRD patterns of Au-Ag@AgCl after recycle.

In Au-Ag@AgCl NCs, the plasmonic absorption of Au nanoparticles was red shifted from 530nm to 520nm. The surface plasmon resonance of the tuber extract was observed at 278 nm, which indicated the presence of polyols in the tubers of *Nephrolepis cordifolia* (Figure1b).[58] The Au-Ag@AgCl NCs were found to be stable for 2 months when the same surface plasmon resonance at 520 nm was observed.

Powder X-ray diffraction analysis was carried out to determine the crystal structure and phase of the Au-Ag@AgCl NCs. XRD pattern confirmed the presence of Au-Ag with AgCl (Figure 1c). Braggs peaks of Au-Ag observed at 38.2^{o}, 44.4^{o}, 64.6^{o}, 77.6^{o} and 81.7^{o}, which indexed with the (111), (200), (220), (311), and (222) planes, respectively, of face-centered cubic Au (JCPDS No. 04-0784) and Ag (JCPDS No. 04-0783).[59] Similarly, XRD peaks at 27.8^{o}, 32.2^{o}, 46.2^{o}, 54.8^{o}, 57.4^{o}, 67.4^{o}, 74.4^{o}, 76.7^{o} and 85.7^{o} were assigned to the (111), (200), (220), (311), (222), (400), (331), (420) and (422) crystal planes, respectively, of crystalline AgCl (JCPDS file : 31-1238).[59,60]

FT-IR analysis was performed in order to identify the capping agents and functional groups responsible for the formation of NCs. Figure 2a shows the FT-IR spectra of the tuber extract and Au-Ag@AgCl NCs. The major absorption peaks of the tuber extract and Au-Ag@AgCl NCs were observed at 3300 cm^{-1}, 2918 cm^{-1}, 1610 cm^{-1}, 1349 cm^{-1}, 1042 cm^{-1}, 527 cm^{-1} and at 3280 cm^{-1}, 2918 cm^{-1}, 1636 cm^{-1}, 1365 cm^{-1}, 1016 and 569 cm^{-1}, respectively (Figure 2a). These absorptions were slightly shifted for Au-Ag@AgCl NCs though the peak at 2918 cm^{-1} remained unchanged. The appearance of absorption peak at ~3300 cm^{-1} was assigned to the O–H stretch of alcohols or phenols and the N–H stretch observed in tuber extract, which moved slightly to 3280 cm^{-1} in Au-Ag@AgCl NCs. Similarly, absorption bands at ~1610 cm^{-1} and

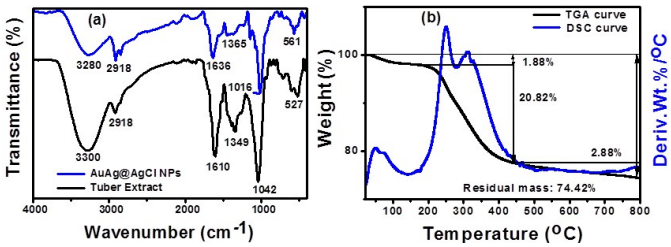

Fig. 2 (a) FT-IR spectra of tuber extract and Au-Ag@AgCl NCs and (b) TGA and DSC curve of and Au-Ag@AgCl NCs.

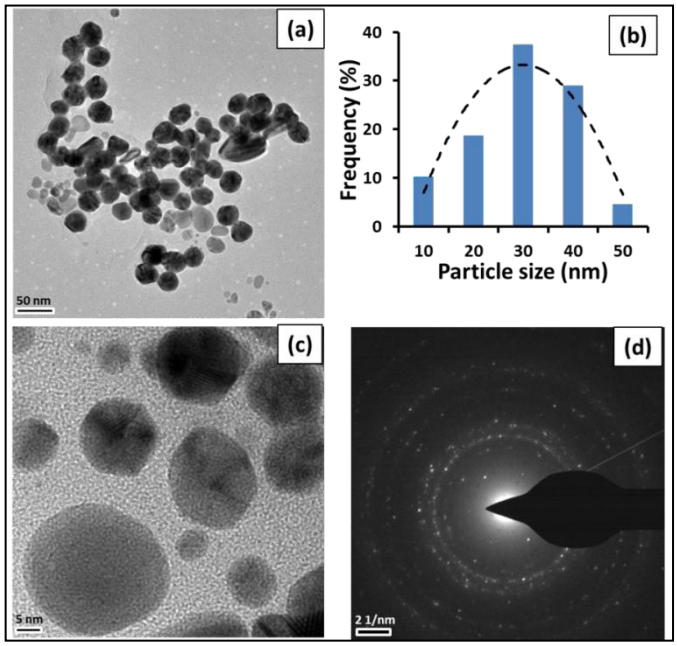

Fig. 3 TEM images of Au-Ag@AgCl NCs (a) at scale bar 50 nm, (b) size distribution histogram (c) at 5 nm scale bar and (d) SAED pattern

1349 cm^{-1} were assigned to asymmetric stretch of C=C and symmetric stretch of C–O, which shifted to 1635 cm^{-1} and 1365 cm^{-1}, presumably due to the presence of other biomolecules in the tuber extract. The absorption peak at 2918 cm^{-1} corresponded to C–H stretch. Slight shifting of peaks in IR absorption bands corresponding to -OH and -NH_2 functional groups was caused by their participation in the reduction and capping of Au-Ag@AgCl NCs. Moreover, ^{1}H NMR analysis of crude $CHCl_3$ extract of *Nephrolepis cordifolia* shows the characteristic peaks of hydroxyl and amine groups at δ 9-12 and 4-5 ppm region (Figure S6 ESI†).

A number of phytochemicals, such as, ethyl palmitate, ethyl linolenate, *β*-ionone, phytol, diterpene alcohol, eugenol, anethol and α-cadinol have been reported in *Nephrolepis cordifolia*.[36] These polyols and flavonoids played the key role for the reduction and capping of Au-Ag@AgCl NCs.

Thermogravimetric analysis was performed to examine the thermal stability of Au-Ag@AgCl NCs produced. Figure 2b presents differential scanning calorimetry- thermogravimetric analysis (DSC–TGA) results for percentage of weight losses while heating from room temperature to 800 °C at 10 °C min^{-1} under N_2. The overall weight loss was found to be 25.58%. Percentage mass losses were observed to occur in three stages. First, the removal of 1.88% by weight around 100°C corresponding to the evaporation of moisture and volatile compounds in the nanocomposite. Second, 20.82% weight loss was observed at ~150 °C to 400 °C, which may have been due to the loss of capping agents present in the bio synthesized Au-Ag@AgCl NCs. Third, 2.88% weight loss occurred beyond 800 °C, which may be due to removal of phytochemicals present in Au-Ag@AgCl NCs. Overall loss in mass along with prominent endothermic peaks at 51.59, 252.17 and 312.53°C were observed in TGA graph. After testing the residue amounted to 74.42% of the original weight of Au-Ag@AgCl NCs, which represented the total amount of Au, Ag and AgCl present.

Au-Ag@AgCl NC particle morphology and size were determined by TEM. Figure 3 shows a TEM image, size distribution histogram, HR-TEM, and SAED patterns of the Au-Ag@AgCl NCs. Most of the nanocomposites were spherical though a few hexagonal particles were also observed (Figure 3a). TEM micrographs showed polydispersed particles sized from 10 to 50 nm and average diameter 30 nm (Figure 3b).

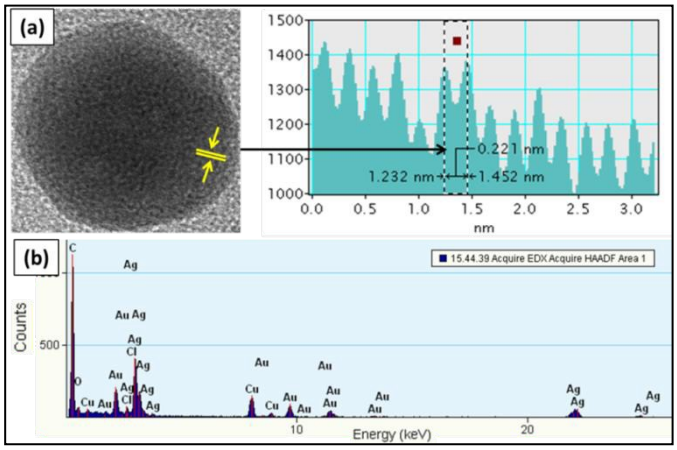

Fig. 4 (a) HRTEM image at 2 nm with d-spacing (b) EDS peaks of Au-Ag@AgCl NCs.

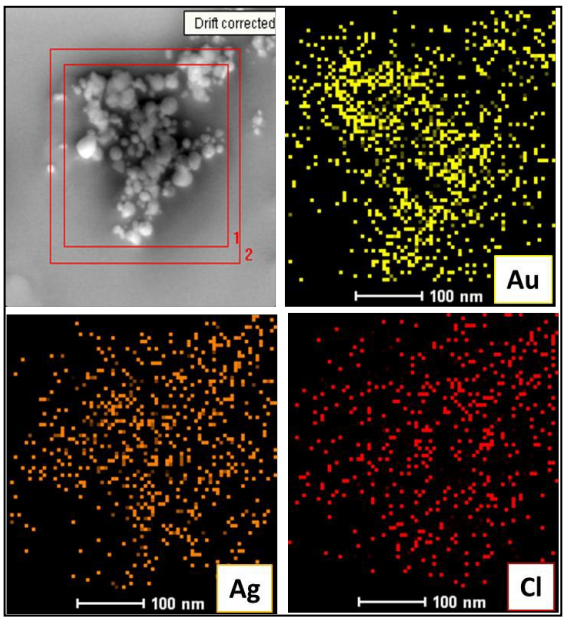

Fig. 5 HAADF-STEM image at 100 nm with the EDS elemental mapping of Au, Ag and Cl

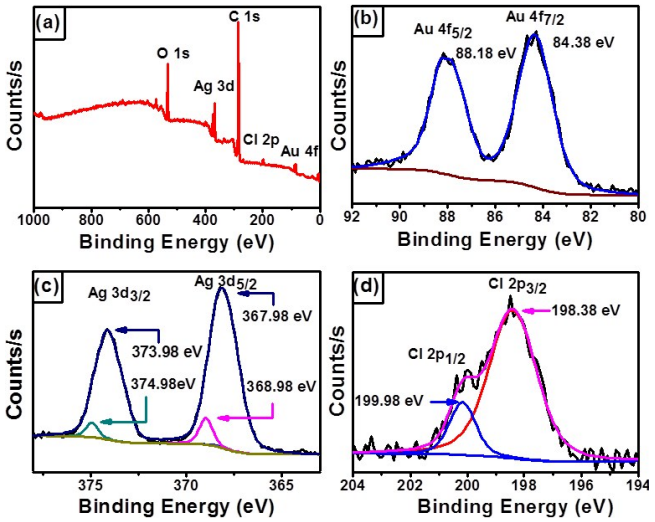

Fig. 6 XPS full scan survey showing (a) Au-Ag@AgCl NCs, (b) Au 4f-electrons of gold, (c) Ag 3d-electrons of silver, and (d) Cl 2p-electrons of Cl.

Figure 3c showed the HRTEM image of the nanocomposite (scale bar =5 nm). The SAED (selected area diffraction) pattern demonstrated the crystalline nature of bio-synthesized Au-Ag @AgCl NCs by the presence of multiple diffraction rings (Figure 3d). Figure 4a shows the HRTEM image with d-spacing of 0.221 nm and EDS confirmed the presence of Au, Ag, Cl, Cu (from the grid), C and O (from biomoleules) (Figure 4b). The high-angle annular dark-field image along with scanning transmission electron microscopy (HAADF-STEM) results showed the elemental mapping of Au, Ag and Cl in the Au-Ag@AgCl NCs (Figure 5).

X-ray photoelectron spectroscopy (XPS) was carried out in order to determine the oxidation state and surface chemical composition of the as synthesized Au-Ag@AgCl NCs (Figure 6). Figure 6a displays the XPS spectrum of Au-Ag@AgCl NCs, which confirmed that the synthesized nanocomposite contains gold, silver and chloride. The presence of C and O in the XPS spectrum could be due to XPS instrumentation and bioorganic molecule present in Au-Ag@AgCl NCs. The XPS peak at 285 eV corresponds to the C 1s region (Fig. S1, ESI†). Figure 6b exhibits the characteristic 4f bands of metallic gold. The doublet peaks represent Au $4f_{7/2}$ and Au $4f_{5/2}$ at binding energies 84.38 and 88.18 eV respectively. The 4f bands were splited into a pair of peaks with a prominent spectrum of $4f_{7/2}$ at a binding energy 84.38 eV, which is characteristic of Au^{o}.[61,62] The two XPS peaks observed at 367.98 eV and 373.98 eV corresponded to Ag $3d_{5/2}$ and Ag $3d_{3/2}$ for Ag^{+} of AgCl respectively (Figure 6c), which was also confirmed by XRD. Furthermore, two small peaks observed at 368.98 eV and 374.98 eV confirmed the binding energies of Ag $3d_{5/2}$ and Ag $3d_{3/2}$ respectively due to metallic silver (Ag^{0}). Previous studies have produced similar results.[63-64] Moreover, figure 6d shows chlorine 2p bands at the binding energies of 198.38 eV and 199.98 eV, corresponding to characteristic Cl $2p_{3/2}$ and Cl $2p_{1/2}$ peaks, respectively.[63] This result further confirmed the presence of Au, Ag^{o}, Ag^{+} and Cl in the synthesized Au-Ag@AgCl NCs.

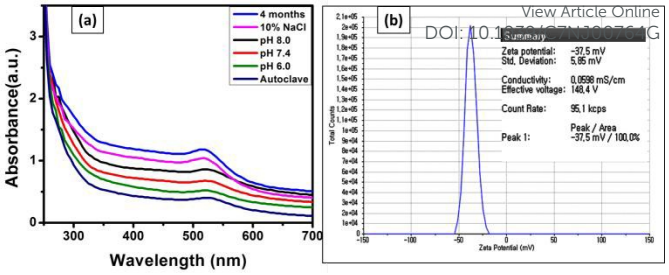

Fig. 7 (a) UV–vis spectra under various parameters (after 4 months, 10%NaCl, pH 8.0, pH 7.4, pH 6.0, and autoclave) and (b) Zeta potential distribution, of the Au-Ag@AgCl NCs

Stability testing of Au-Ag@AgCl NCs

The stability of *Nephrolepis cordifolia* stabilized Au-Ag@AgCl NCs was studied by evaluating the plasmon resonance (SPR) peaks using various parameters. For example, the plasmon wavelength measured after 4 months, using 10% NaCl, autoclaved at 120 ^{o}C for 50 minutes and in phosphate buffer solution at pH 6, 7.4 and 8 shows only slight shift of λmax (1 – 5 nm). These results demonstrate that Au-Ag@AgCl NCs were stable in biological fluids at physiological pH (Figure 7a). Moreover, zeta potential distribution Au-Ag@AgCl NCs in aqueous solution was found to be -37.5 mV (Figure 7b). Thus large negative zeta potential value confirmed the higher stability of Au-Ag@AgCl NCs.[65,66]

Catalytic activity

The selection and optimization of the catalyst is presented in Table 1. The highest yield of the product **4a** was obtained using Au-Ag@AgCl NCs compared to other catalysts such as AuNPs, AgNPs, $AgNO_3$, $HAuCl_4$ and plant extract. Based on the optimization study, quinolines **4a**-**4f** were synthesized by tandem annulation/aromatization of aryl aldehydes (**1a** or **1b**) and aniline derivatives (**2a** or **2b**) with various phenyl acetylene derivatives (**3a**-**3d**) as summarized in Table 2. Reaction of benzaldehyde (**1a**) and aniline (**2a)** in the presence of phenyl acetylene (**3a**) and 2 mol% Au-Ag@AgCl NCs in refluxing 1,2-dichloroethane (DCE) for 9 h provided **4a** in 96% yield (entry 1, Table 2). Reaction between 4-methyl benzaldehyde (**1b)** and aniline (**2a**) in the presence of phenyl acetylene (**3a**) afforded product **4b** in 97% yield (entry 2, Table 2). Similarly, diversely substituted phenyl acetylenes 1-ethynyl-3-methylbenzene (**3b**), 1-chloro-3-ethynylbenzene (**3c**), or 1-ethynylnaphthalene (**3d**) reacted with **1a** and **2b** in refluxing DCE to afford the desired products **4c**-**4e** in 95, 96 and 93% yields, respectively (entries 3-5, Table 2). Moreover, reaction between naphthalen-1-amine (**2b**) and **1a** and **3a** provided 2,4-diphenylbenzo[*h*]quinoline (**4f**) in 91% yield. These results show the Au-Ag@AgCl NCs provide efficient synthetic routes to biologically interesting heterocycles in good yield. The structure of **4a** was identified by ^{1}H and ^{13}C NMR and by direct comparison with reported data (data and spectra of the synthesized compounds are presented in the ESI†).

Table 1 Optimization of the reaction conditions for the synthesis of **4a**[a]

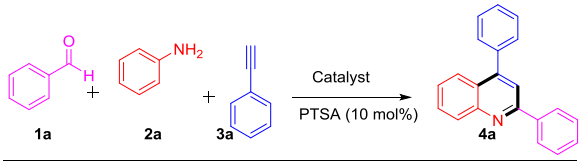

Entry	Catalyst	Solvent	Conditions	Yield (%)[b]
1	AuNPs	DCE	12 h, reflux	43
2	AgNPs	DCE	12 h, reflux	30
3	$AgNO_3$	DCE	12 h, reflux	25
4	$HAuCl_4$	DCE	12 h, reflux	25
5	Au-Ag@AgCl NCs	DCE	9 h, reflux	96
6	Au-Ag@AgCl NCs	DCE	9 h, 80 °C	50
7	Tuber extract of *Nephrolepis cordifolia*	DCE	12 h, reflux	0

[a]Reaction conditions: Aldehyde **1** (1.0 mmol), amine **2** (1.0 mmol), alkyne **3** (1.0 mmol), catalyst (2 mol%), PTSA (10 mol%), solvent 1,2-dichloroethane (5.0 mL).

Table 2 Construction of diverse quinoline derivatives from aniline, benzaldehyde and phenyl acetylene derivatives via Au-Ag@AgCl NCs catalyzed multicomponent domino annulation-aromatization[a]

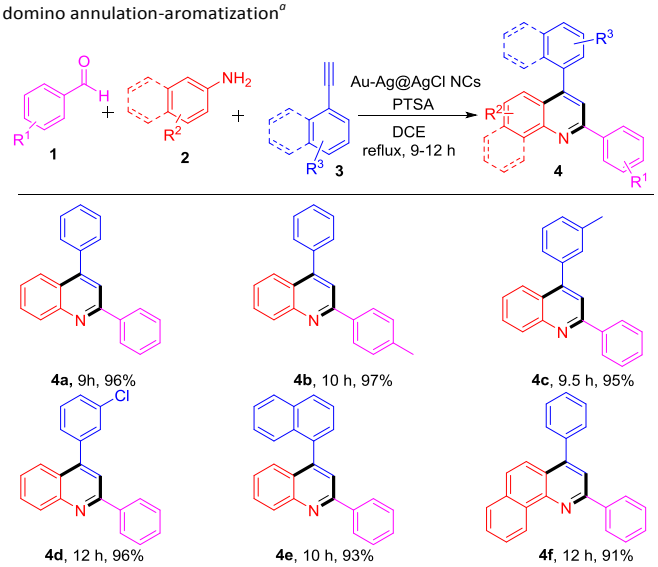

[a]Reaction conditions: Aldehyde **1** (1.0 mmol), amine **2** (1.0 mmol), alkyne **3** (1.0 mmol), Au-Ag@AgCl NCs nanocatalyst (2 mol%), PTSA (10 mol%), solvent 1,2-dichloroethane (5.0 mL).

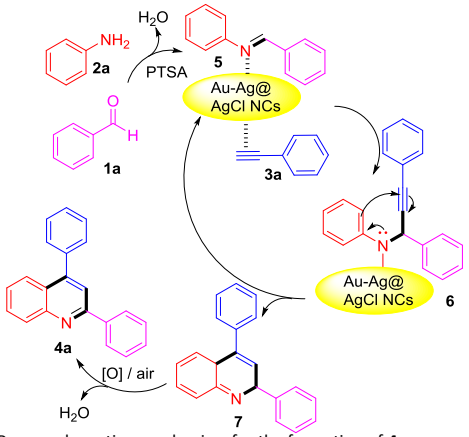

Scheme 2 Proposed reaction mechanism for the formation of **4a**.

Table 3 Recyclability of the Au-Ag@AgCl NCs [a]

View Article Online
DOI: 10.1039/C7NJ00764G

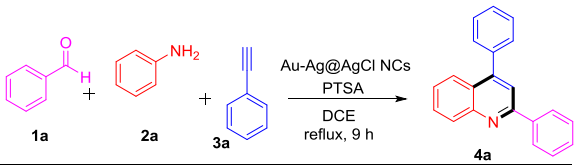

Entry	Cycle	Yield (%)[b]
1	First	96
2	Second	95
3	Third	93
4	Fourth	91
5	Fifth	88

[a]Reaction conditions: Aldehyde **1a** (1.0 mmol), amine **2a** (1.0 mmol), alkyne **3a** (1.0 mmol), Au-Ag@AgCl NCs nanocatalyst (2 mol%), PTSA (10 mol%), solvent 1,2-dichloroethane (5.0 mL), [b]Isolated yield.

Proposed reaction mechanism for the formation of **4a** in the presence of Au-Ag@AgCl NCs is illustrated in Scheme 2. Aldehyde **1a** condenses with amine **2a** in presence of *p*-toluenesulphonic acid (PTSA) to form imine **5**, which forms a coordination complex with Au-Ag@AgCl NCs and alkyne **3a** to produce the propargylamine intermediate **6**. Intermediate **6** then undergoes intramolecular hydroarylation of the alkyne to afford dihydroquinoline intermediate **7**. Finally, air oxidation of intermediate **7** provides the required quinoline **4a**.

Recyclability of catalyst

Catalyst recyclability was examined in order to test the stability of the synthesized Au-Ag@AgCl NCs. For this purpose, a series of recycle experiments were conducted as shown in Table 3. After washing with ethyl acetate and hot water five times and drying in vacuum for 3 h, recovered Au-Ag@AgCl NCs were recycled. Au-Ag@AgCl NC was recycled and reused for five times without significance loss of catalytic activity. XRD analysis of the Au-Ag@AgCl NCs after recycling

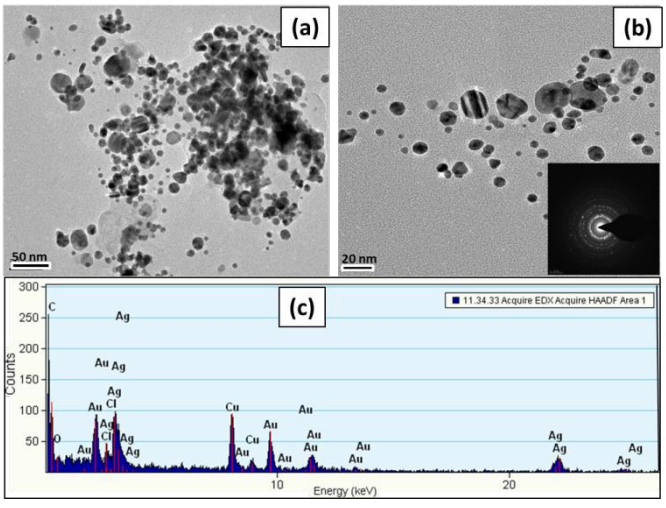

Fig. 8 TEM images of recycled Au-Ag@AgCl NCs at scale bar (a) 50 nm (b) 20 nm (inset: SAED pattern), and (c) EDS peaks after 5th catalytic cycle.

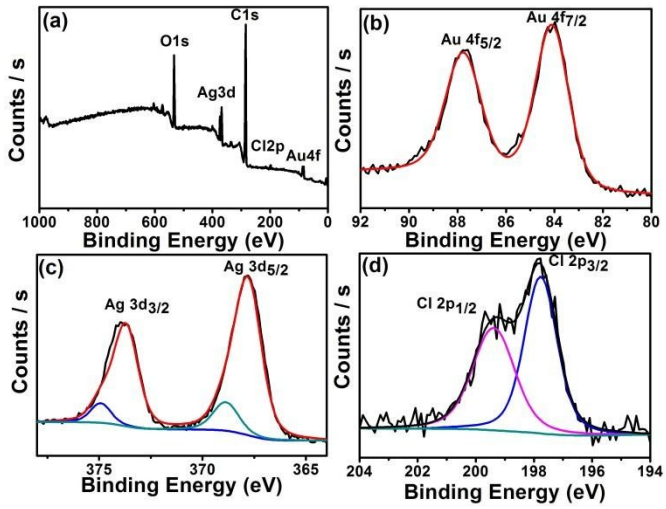

Fig. 9 (a) XPS full scan survey, (b) Au 4f-electrons of gold, (c) Ag 3d-electrons of silver, and (d) Cl 2p-electrons of Cl of recycled Au-Ag@AgCl NCs after 5th cycle.

five times produced identical XRD patterns (Figure 1d). In addition, there is no any alteration in elemental composition and surface chemistry of the recycled Au-Ag@AgCl NCs, which was further established by TEM (Figure 8) HAADF-STEM elemental mapping (Figure S3 ESI†) and XPS spectra (Figure 9), respectively, after 5 consecutive cycles.

Conclusions

An environmental friendly method was developed for the efficient synthesis of Au-Ag@AgCl NCs using the tuber extract of *Nephrolepis cordifolia*, which was used as a reducing and stabilizing agent. The formation of crystalline small sized (10-50 nm), well dispersed nanocomposites were confirmed by powder X-ray diffraction (XRD) and transmission electron microscopy (TEM). Elemental composition and oxidation states of nanocomposites were investigated by energy-dispersive X-ray (EDX) spectroscopy and XPS analysis. The synthetic utility of the synthesized Au-Ag@AgCl NCs was demonstrated by synthesizing pharmaceutically important quinoline derivatives in excellent yield via multicomponent tandem annulation/aromatization reaction of aldehydes, amines, and alkynes. Moreover, the Au-Ag@AgCl NCs produced displayed excellent catalytic activities and good recyclability. Thus, we believe the additive free Au-Ag@AgCl nanocomposites described could be used as green, sustainable, and efficient catalysts for organic transformation.

Acknowledgements

This work was supported by a Yeungnam University Research Grant (2017).

Notes and references

View Article Online
DOI: 10.1039/C7NJ00764G

1 P. Kuppusamy, S. J. A. Ichwan, P. N. H. Al-Zikri, W. H. Suriyah, I. Soundharrajan, N. Govindan, G. P. Maniam and M. M. Yusoff, *Biol. Trace. Elem. Res.*, 2016, **173**, 297.
2 V. Malapermal, J. N. Mbatha, R. M. Gengan and K. Anand, *Adv. Mater. Lett.* 2015, **6**, 1050.
3 K. Bankura, D. Maity, M. M. R. Mollick, D. Mondal, B. Bhowmick, I. Roy, T. Midya, J. Sarkar, D. Rana, K. Acharya and D. Chattopadhyay, *Carbohydr. Polym*., 2014, **107**, 151.
4 S. P. Velammal, T. A. Devi and T. P. Amaladhas, *J. Nanostruct. Chem.*, 2016, **6**, 247.
5 R. Kaegi, A. Voegelin, B. Sinnet, S. Zuleeg, H. Hagendorfer, M. Burkhardt and H. Siegrist, *Environ. Sci. Technol.*, 2011, **45**, 3902.
6 P. Mukherjee, A. Ahmad, D. Mandal, S. Senapati, S. R. Sainkar, M. I. Khan, R. Ramani, R. Parischa, P. V. Ajayakumar, M. Alam, M. Sastry and R. Kumar, *Angew. Chem., Int. Ed.*, 2001, **40**, 3585.
7 S. W. Lee, C. Mao, C. E. Flynn and A. M. Belcher, *Science*, 2002, **296**, 892.
8 J. Virkutyte and R. S. Varma, *Chem. Sci.*, 2011, **2**, 837.
9 J. Kou and R. S. Varma, *ChemSusChem*, 2012, **5**, 2435.
10 M. Kowshik, S. Ashtaputre, S. Kharrazi, W. Vogel, J. Urban , S. K. Kulkarni and K. M. Paknikar, *Nanotechnology*, 2003, **14**, 95.
11 P. Raveendran, J. Fu and S. L. Wallen, *Green Chem.*, 2006, **8**, 34.
12 P. Dauthal and M. Mukhopadhyay, *Ind. Eng. Chem. Res.*, 2016, **55**, 9557.
13 V. Kumar and S. K. Yadav, *J. Chem. Technol. Biotechnol.*, 2009, **84**, 151.
14 F. Lu, D. Sun, J. Huang, M. Du, F. Yang, H. Chen, Y. Hong, and Q. Li, *ACS Sustainable Chem. Eng.*, 2014, **2**, 1212.
15 K. Mishra, T. N. Poudel, N. Basavegowda and Y. R. Lee, *J. Catal.*, 2016, **344**, 273.
16 S. Iravani, Green Chem., 2011, **13**, 2638.
17 M. Shah , D. Fawcett, S. Sharma , S. K. Tripathy and G. E. J. Poinern, *Materials*, 2015, **8**, 7278.
18 M. Naghdi, M. Taheran, S. K. Brar, M. Verma, R. Y. Surampalli and J. R. Valero, *Beilstein J. Nanotechnol.,* 2015, **6**, 2354.
19 C. Burda, X. Chen, R. Narayanan and M. A. El-Sayed, *Chem. Rev.*, 2005, **105**, 1025.
20 F. Tao, M. E. Grass, Y. Zhang, D. R. Butcher, J. R. Renzas, Z. Liu, J. Y. Chung, B. S. Mun, M. Salmeron and G. A. Somorjai, *Science*, 2008, **322**, 932.
21 J. A. Rodriguez and D. W. Goodman, *Science*, 1992, **257**, 897.
22 R. Ferrando, J. Jellinek and R. L. Johnston, *Chem. Rev.*, 2008, **108**, 845.
23 Q. Cao, K. Yuan, Q. Liu, C. Liang, X. Wang, Y.-F. Cheng, Q. Li, M. Wang and R. Che *ACS Appl. Mater. Interfaces*, 2015, **7**, 18491.
24 J. H. Shim, J. Yang, S.-j. Kim, C. Lee and Y. Lee, *J. Mater. Chem*., 2012, **22**, 15285.
25 R. Liu, J. Guo, G. Ma, P. Jiang, D. Zhang, D. Li, L. Chen, Y. Guoand, G. Ge, *ACS Appl. Mater. Interfaces*, 2016, **8**, 16833.
26 S. Liu, G. Chen, P. N. Prasad and M. T. Swihart, *Chem. Mater*., 2011, **23**, 4098.
27 A. K. Samal, L. Polavarapu, S. Rodal-Cedeira, L. M. Liz-Marzán, J. Pérez-Juste and I. Pastoriza-Santos, *Langmuir*, 2013, **29**, 15076.
28 A. G. Garcia, P. P. Lopes, J. F. Gomes, C. Pires, E. B. Ferreira, R. G. M. Lucena, L. H. S. Gasparotto and G. Tremiliosi, *New J. Chem.*, 2014, **38**, 2865.
29 P. Hu, X. Hu, C. Chen, D. Hou and Y. Huang, *CrystEngComm*, 2014, **16**,649.
30 J. Jiang, and L. Zhang, Chem.-Eur. J., 2011, **17**, 3710.

31 R. Dong, B. Tian, C. Zeng, T. Li, T. Wang and J. Zhang, *J. Phys. Chem. C*, 2013, **117**, 213.
32 H. Daupor and S. Wongnawa, *Mater. Chem. Phys.*, 2015, **159**, 71.
33 H. Shi, J. Chen, G. Li, X. Nie, H. Zhao, P.-K. Wong and T. An, *ACS Appl. Mater. Interfaces*, 2013, **5**, 6959.
34 W. Yan, X. Feng, X. Chen, W. Hou, J.-J. Zhu, *Biosens. Bioelectron.*, 2008, **23**, 925.
35 T. B. Devi, M. Ahmaruzzaman and S. Begum, *New J. Chem.,* 2016, **40**, 1497.
36 M. E. El-Tantawy, M. S. Afifi and M. M. Shams, *Can. J. Pure Appl. Sci.*, 2015, **9**, 3365.
37 A. A. AbdelHamid, M. A. Al-Ghobashy, M. Fawzy, M. B. Mohamed and M. M. S. A. Abdel-Mottaleb, *ACS Sustainable Chem. Eng.,* 2013, **1**, 1520.
38 A. I. Lukman, B. Gong, C. E. Marjo, U. Roessner, A. T. Harris, *J. Colloid Interface Sci.*, 2011, **353**, 433.
39 J. P. Michael, *Nat. Prod. Rep.*, 2008, **25**, 166.
40 G. Francio, F. Faraone and W. Leitner, *Angew. Chem., Int. Ed.*, 2000, **39**, 1428.
41 H. U. Blaser, H. P. Jalett, W. Lottenbach and M. Studer, *J. Am. Chem. Soc.*, 2000, **122**, 12675.
42 C. J. Tonzola, A. P. Kulkarni, A. P. Gifford, W. Kaminsky, and S. A. Jenekhe, *Adv. Funct. Mater.*, 2007, **17**, 863.
43 A. P. Kulkarni, C. J. Tonzola, A. Babel and S. A. Jenekhe, *Chem. Mater.*, 2004, **16**, 4556.
44 A. C. Grimsdale, K. L. Chan, R. E. Martin, P. G. Jokisz and A. B. Holmes, *Chem. Rev.*, 2009, **109**, 897.
45 M. V. N. de Souza, K. C. Pais, C. R. Kaiser, M. A. Peralta, M. de L. Ferreira and M. C. S. Lourenco, *Bioorg. Med. Chem.*, 2009, **17**, 1474.
46 B. Heiniger, G. Gakhar, K. Prasain, D. H. Hua and T. A. Nguyen, *Anticancer Res.* 2010, **30**, 3927.
47 J. L. McCormick, T. C. McKee, J. H. Cardellina and M. R. Boyd, *J. Nat. Prod*., 1996, **59**, 469.
48 M. Foley and L. Tilley, *Int. J. Parasitol.*, 1997, **27**, 231.
49 A. K. Nedeltchev, H. Han and P. K. Bhowmik, *Tetrahedron*, 2010, **66**, 9319.
50 J. P. Bridhkoti, R. Gahlaut, H. C. Joshi and S. Pant, *J. Lumin.*, 2011,**131**, 1869.
51 K. Pericherla, A. Kumar and A. Jha, *Org. Lett.*, 2013, **15**, 4078.
52 C. E. Meyet and C. H. Larsen, *J. Org. Chem.* 2014, **79**, 9835.
53 Y. Su, M. Lu, B. Dong, H. Chen and X. Shiaj, *Adv. Synth. Catal.,* 2014, **356**, 692.
54 S. Kaur, M. Kumar and V. Bhalla, *Chem. Commun.,* 2015, **51**, 16327.
55 K. Cao, F.-M. Zhang, Y.-Q. Tu, X.-T. Zhuo and C.-A. Fan, *Chem.-Eur. J.*, 2009, **15**, 6332.
56 S. M. Prajapati, K. D. Patel, R. H. Vekariya, S. N. Panchal and H. D. Patel, *RSC Adv.*, 2014, **4**, 24463.
57 V. V. Kouznetsov, L. Y. Mendez and C. M. Gomez, *Curr. Org. Chem.*, 2005, **9**, 141.
58 K. Mishra, N. Basavegowda and Y. R. Lee, *Appl. Catal., A,* 2015**, 506,** 180.
59 Q. Cao, K. Yuan, Q. Liu, C. Liang, X. Wang, Y.F. Cheng, Q. Li, M. Wang and R. Che, *ACS Appl. Mater. Interfaces*, 2015, **7**, 18491−18500
60 B. Ma, J. Guo, W.-L. Dai and K. Fan, *Appl. Catal., B*, 2013, **130– 131**, 257.
61 A. Pearson, A. P. O'Mullane, V. Bansal and S. K. Bhargava, *Inorg. Chem.*, 2011, **50**, 1705.
62 B. Wang, M. Zhang, W. Li, L. Wang, J. Zheng, W. Gan and J. Xu, *Dalton Trans*., 2015, **44**, 17020.
63 P. Wang, B. Huang, Z. Lou, X. Zhang, X. Qin, Y. Dai, Z. Zheng and X. Wang, *Chem.-Eur. J*., 2010, **16**, 538.
64 Z. Xu and S-Y. Lin, *RSC Adv*., 2016, **6**, 84738.
65 K. Sapkota, K. B. Narayanan, and S. S. Han. *J. Clust. Sci*., 2017, **28**, 1605.
66 A. Ahmad, Y. Wei, F. Syed, M. Imran, Z. U. H. Khan, K. Tahir, A. U. Khan, M. Raza, Q. Khana and Q. Yuan, *RSC Adv*., 2015, **5**, 99364.